Kinetics and Mechanism of the Hydration of CO_2 and Dehydration of HCO_3^- Catalyzed by a Zn(II) Complex of 1,5,9-Triazacyclododecane as a Model for Carbonic Anhydrase

Xiaoping Zhang,[†,‡] Rudi van Eldik,*[,†] Tohru Koike,[§] and Eiichi Kimura[§]

Institute for Inorganic Chemistry, University of Witten/Herdecke, Stockumer Strasse 10, 58448 Witten, Germany, and Department of Medicinal Chemistry, Hiroshima University School of Medicine, Hiroshima University, Kasumi 1-2-3, Minami-ku, Hiroshima 734, Japan

Received June 9, 1993[⊗]

A detailed kinetic study of the hydration of CO_2 and dehydration of HCO_3^- was performed in the absence and presence of a model Zn(II) complex for carbonic anhydrase. The Zn(II) complex of 1,5,9-triazacyclododecane ([12]aneN$_3$) was found to catalyze both the hydration of CO_2 and dehydration of HCO_3^-. The pH dependence of these reactions clearly demonstrates that it is only the hydroxo form of the complex that catalyzes the hydration reaction via CO_2 uptake by coordinated hydroxide, whereas it is only the aqua complex that catalyzes the dehydration of HCO_3^- via a ligand substitution process. The kinetic data reveal acid dissociation constants (expressed as pK_a values) of 7.45 ± 0.10 and 7.29 ± 0.13 from the hydration and dehydration reactions, respectively, which are in excellent agreement with the thermodynamically determined value of 7.5 for the model Zn(II) complex. The second-order rate constants for the catalytic reaction paths are 581 ± 64 and 4.8 ± 0.7 M^{-1} s^{-1} at 25 °C for the hydration of CO_2 and dehydration of HCO_3^-, respectively. The results are discussed in reference to data available for other model systems and carbonic anhydrase itself.

Introduction

The mode of action and the role of Zn in the catalytic mechanism of carbonic anhydrases have received significant attention from numerous experimentalists and theoreticians over the last few years.[1-12] The carbonic anhydrases (CA) are zinc containing metalloenzymes that catalyze the reversible hydration of CO_2 and dehydration of HCO_3^- given in (1). Three of the

$$CO_2 + H_2O \rightleftharpoons HCO_3^- + H^+ \qquad (1)$$

seven distinct observed isozymes have high turnover numbers (between 10^4 and 10^6),[10] and therefore the nature of the active site has been a topic of great interest. X-ray diffraction studies have revealed the active site environment for human carbonic anhydrase B and C, which is given in Scheme I.[8] The active site is ca. 15 Å across and 15 Å deep, and has a zinc ion positioned at its bottom. The zinc atom is bound to three histidine imidazole groups (His-96, -94, and -119) in a distorted tetrahedral array, with the fourth site occupied by either a water molecule or a hydroxide ion hydrogen bonded to Thr-199, which is itself hydrogen bonded to Glu-106 as shown in Scheme I. The enzyme site can be divided into hydrophilic and hydrophobic halves. The hydrophilic half contains the proton acceptor group His-64 and partially ordered water molecules. His-64 is thought to be important for the shuttling of protons out of the active cavity.[13] The ordered water molecules in the active cavity are thought to be important for the intramolecular transfer of protons from the zinc-bound water to His-64. In the hydrophobic half, a "deep" water molecule close to the zinc center is thought to be important for CO_2 recognition. The catalytic activity of CA is characterized by a pK_a value of ca. 7, such that hydration of CO_2 is dominant above pH 7, while the dehydration of HCO_3^- is observed below pH 7.[2] It has been postulated that this pK_a value represents that of the coordinated water molecule on the Zn center that participates in the catalytic reaction as summarized in (2)[3] and shown in Scheme II.[8]

$$EZnH_2O \rightleftharpoons EZnOH^- + H^+$$

$$EZnOH^- + CO_2 \rightleftharpoons EZnHCO_3^- \qquad (2)$$

$$EZnHCO_3^- + H_2O \rightleftharpoons EnZnH_2O + HCO_3^-$$

One of the approaches adopted to resolve the nature of the active site in CA has been to design various types of metal complexes to account for or to mimic the functions of the central Zn(II) ion. Studies in recent years have focused on model complexes of Co(III),[14,15] Cu(II),[16,17] and Zn(II).[18-29] In the

* Address correspondence to this author at the University of Witten/Herdecke.
† University of Witten/Herdecke.
‡ On leave from the Institute of Molecular Science, Shanxi University, Taiyuan, Shanxi, P.R. China.
§ Hiroshima University School of Medicine.
⊗ Abstract published in *Advance ACS Abstracts*, October 15, 1993.

(1) Coleman, J. E. In *Zinc Enzymes*, Bertini, I., Luchinat, C., Maret, W., Zeppezauer, M., Eds.; Birkhauser: Boston, MA, 1986; p 49; see also Chapters 22–26.
(2) Botré, F.; Gros, G.; Storey, B. T. *Carbonic Anhydrase* VCH: Weinheim, Germany, 1991.
(3) Silverman, D. N.; Lindskog, S. *Acc. Chem. Res.* **1988**, *21*, 30.
(4) Kassebaum, J. W.; Silverman, D. N. *J. Am. Chem. Soc.* **1989**, *111*, 2691.
(5) Pocker, Y.; Janjic, N. *J. Am. Chem. Soc.* **1989**, *111*, 731.
(6) Krauss, M.; Garmer, D. R. *J. Am. Chem. Soc.* **1991**, *113*, 6426.
(7) Garmer, D. R.; Krauss, M. *J. Am. Chem. Soc.* **1992**, *114*, 6487.
(8) Merz, K. M.; Hoffmann, R.; Dewar, M. J. S. *J. Am. Chem. Soc.* **1989**, *111*, 5636.
(9) Merz, K. M. *J. Am. Chem. Soc.* **1991**, *113*, 406.
(10) Merz, K. M.; Murcko, M. A.; Kollman, P. A. *J. Am. Chem. Soc.* **1991**, *113*, 4484.
(11) Sola, M.; Lledos, A.; Duran, M.; Bertran, J. *Inorg. Chem.* **1991**, *30*, 2523; *J. Am. Chem. Soc.* **1992**, *114*, 869.
(12) Jacob, O.; Cardenas, R.; Tapia, O. *J. Am. Chem. Soc.* **1990**, *112*, 8692.
(13) Zheng, Y.-J.; Merz, K. M. *J. Am. Chem. Soc.* **1992**, *114*, 10498.
(14) Groves, J. T.; Baron, L. A. *J. Am. Chem. Soc.* **1989**, *111*, 5442.
(15) Chin, J.; Banaszczyk, M. *J. Am. Chem. Soc.* **1989**, *111*, 2724.
(16) Hay, R. W.; Basak, A. K.; Pujari, M. P. *J. Chem. Soc., Dalton Trans.* **1989**, 197.
(17) Chin, J.; Jubian, V. *J. Chem. Soc., Chem. Commun.* **1989**, 839.
(18) Gellman, S. H.; Petter, R.; Breslow, R. *J. Am. Chem. Soc.* **1986**, *108*, 2388.
(19) Iverson, B. L.; Lerner, R. A. *Science* **1989**, *243*, 1185.
(20) Kimura, E.; Shiota, T.; Koike, T.; Shiro, M.; Kodama, M. *J. Am. Chem. Soc.* **1990**, *112*, 5805.
(21) Koike, T.; Kimura, E. *J. Am. Chem. Soc.* **1991**, *113*, 8935.

0020-1669/93/1332-5749$04.00/0

Scheme I

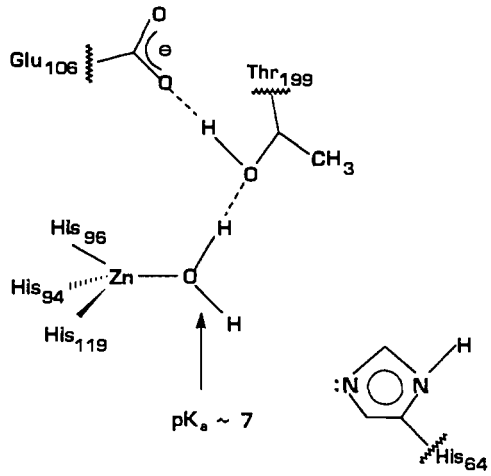

case of model Zn(II) complexes, there are six species summarized in Scheme III that exhibit interesting structural and thermodynamic properties to serve in model studies on the behavior of CA. Of these, the macrocyclic tetraamine complex **1**,[18] the cyclen complex **2**,[25] the [12]aneN$_3$ complex **4**,[20] and the tris(imidazolyl) complex **5** (R_1, R_2, R_3 = $CH(CH_3)_2$; Y = Cl^-) are structurally well defined. Complexes **1**–**4** are H_2O-bound Zn(II) complexes that all generate L–Zn^{II}–OH species with pK_a(H_2O) values of 8.7,[18] 8.0,[25] 8.3,[21] and 7.3,[20] respectively. The pH dependence of the observed rate constants for the hydrolysis of neutral phosphotriesters implied that the L–Zn^{II}–OH species represent the active form of the model complexes. In contrast, complexes **5** and **6** did not show this behavior. It follows that complexes **5** and **6** did not show this behavior. It follows that complexes **1**–**4** are likely to be suitable models to mimic the nucleophilic attack of substrates on the OH^--coordinated Zn(II) center. An important question is whether the distorted four coordinate geometry and low pK_a of ca. 7 for the coordinated water molecule play an important role during the nucleophilic attack. Complex **4** has a tridentate ligand and is reported to be structurally and chemically the best model for CA (Scheme I) to date. It exhibits a pK_a value of 7.3, which is almost identical with that for CA. Furthermore, in the OH^- form it catalyzes the hydration of acetaldehyde and the hydrolysis of carboxylic esters.[20,21] Another surprising property of **4** is that the anion binding affinity is very similar to or even better than for CA.[20,22,23] All these outstanding properties made complex **4** an ideal candidate to study its catalytic effect on the hydration of CO_2 and the dehydration of HCO_3^-. In addition, our earlier experience with kinetic and mechanistic studies of CO_2 uptake and decarboxylation reactions of model transition metal complexes[30,31] provided the appropriate background for these investigations.

Experimental Section

Materials. All reagents used were of analytical reagent grade. The model complex **4**, ([12]aneN$_3$-Zn^{II}-OH)$_3$(ClO_4)$_3$·$HClO_4$, was prepared and characterized as described before.[20] The following indicators and biological buffers were purchased and used without further purification: chlorophenol red (Sigma), 4-nitrophenol (Merck), phenol red (Merck), *m*-cresol purple (Sigma), thymol blue (Merck), Mes (2-[*N*-morpholino]ethanesulfonic acid, Merck), Bis-tris ((bis[2-hydroxyethyl]imino)-tris[hydroxymethyl]methane, Sigma), Mopso (3-[*N*-morpholino-2-hydroxypropanesulfonic acid, Sigma), Mops (3-[*N*-morpholino]propanesulfonic acid, Sigma), Hepes (*N*-[2-hydroxyethyl]piperazine-*N*′-[2-ethanesulfonic acid], Merck), Hepps (*N*-[2-hydroxyethyl]piperazine-*N*′-[3-propanesulfonic acid], Merck), Taps (*N*-tris[hydroxymethyl]methyl-3-aminopropanesulfonic acid, Sigma), Ampso (3-[(1,1-dimethyl-2-hydroxyethyl)amino]-2-hydroxypropanesulfonic acid, Sigma). All solutions were prepared using distilled and deionized water that was boiled for more than 1.5 h prior to use to remove the dissolved CO_2.

CO_2 solutions (ca. 0.02 M) were prepared via careful acidification of 0.04 M $NaHCO_3$ solutions with 0.04 M $HClO_4$ to a pH between 3.2 and 3.7 monitored on a pH meter. Such solutions could not be stored without loss of CO_2, and were therefore prepared freshly immediately before use and introduced into the syringe of the stopped-flow instrument. HCO_3^- solutions (ca. 0.012 M) were freshly prepared from $NaHCO_3$ and used within 12 h. The ionic strength of all test solutions was adjusted to 0.11 M with the aid of $NaClO_4$ for the hydration reaction and to 0.10 M for the dehydration reaction.

Kinetic Procedures. All kinetic measurements were performed at 25.0 ± 0.1 °C on a Durrum D110 stopped-flow instrument attached to an on-line data acquisition and handling system, using the OLIS KINFIT (Jefferson, Ga) set of programs. A Metrohm 632 pH meter equipped with an Ingold V402-S7/120 electrode was connected directly to the receiver reservoir of the stopped-flow instrument in order to determine the pH of the reaction mixture directly after mixing. The reactions were followed using the "change in pH-indicator" method, in which pairs of buffers and indicators having nearly the same pK_a values are employed, as described by Khalifah.[32] Concentrations were selected in such a way that the total buffer concentration was 50 mM after mixing in the stopped-flow. The pK_a values, appropriate wavelengths to study the reaction, and the change in extinction coefficient for the series of buffer–indicator pairs, measured under the same conditions, are as follows: Mes (pK_a = 6.3) and Bis-Tris (pK_a = 6.5) with chlorophenol red (pK_a = 6.3, λ = 574 nm, Δε = 4.71 × 10^4 M^{-1} cm^{-1}); Mopso (pK_a = 6.9) and Mops (pK_a = 7.2) with 4-nitrophenol (pK_a = 7.1, λ = 400 nm, Δε = 1.81 × 10^4 M^{-1} cm^{-1}); Hepes (pK_a = 7.5) with phenol red (pK_a = 7.5, λ = 558 nm, Δε = 6.41 × 10^4 M^{-1} cm^{-1}); Hepps (pK_a = 8.0), Tricine (pK_a = 8.1), and Taps (pK_a = 8.4) with *m*-cresol purple (pK_a = 8.3, λ = 578 nm, Δε = 3.88 × 10^4 M^{-1} cm^{-1}); Ampso (pK_a = 9.0) with thymol blue (pK_a = 8.9, λ = 596 nm, Δε = 2.43 × 10^4 M^{-1} cm^{-1}).

The initial rate, $V_{initial}$, was estimated from eq 3,[33-35] where A_0 and A_e are the initial and final absorbance values, and Q is the buffer factor for

$$V_{initial} = Q(A_0 - A_e)[d(\ln (A - A_e))/dt]_{t\to 0} \quad (3)$$

converting changes in the absorbance of the indicator to changes in CO_2 or HCO_3^- concentration. The values of Q were determined before a series of kinetic measurements and in some cases checked after completion of the measurements. For this purpose, solutions of different concentrations of $HClO_4$ or NaOH, similar to those of CO_2 or HCO_3^-, were mixed with the buffer–indicator solutions in the stopped-flow instrument.[36] The absorbance change was recorded as a function of $HClO_4$ or NaOH concentration, and Q was calculated from the reciprocal slope of a plot of absorbance change versus [$HClO_4$] or [NaOH]. The last term in eq 3 was determined from the initial slope of the absorbance–time trace. Alternatively, it was also calculated from the apparent rate constant using a one exponential fit routine (OLIS, KINFIT) in which 10% of the reaction was taken.

The procedures for a typical kinetic experiment were as follows. One syringe in the stopped-flow was filled with a 100 mM buffer solution containing (2–12) × 10^{-4} M Zn^{II}–[12]aneN$_3$, 0.2 M $NaClO_4$ for the hydration reaction and 0.1 M $NaClO_4$ for the dehydration reaction, and (4–10) × 10^{-5} M indicator (in the case of the reference experiment the solution did not contain the Zn(II) complex). The second syringe was filled with the freshly prepared CO_2 (in 0.02 M $NaClO_4$) or HCO_3^- (in

(22) Kimura, E.; Koike, T. *Comments Inorg. Chem.* **1991**, *11*, 285.
(23) Koike, T.; Kimura, E.; Nakamura, I.; Hashimoto, Y.; Shiro, M. *J. Am. Chem. Soc.* **1992**, *114*, 7338.
(24) Alsfasser, R.; Trofimenko, S.; Looney, A.; Parkin, G.; Vahrenkamp, H. *Inorg. Chem.* **1991**, *30*, 4098.
(25) Norman, P. R. *Inorg. Chim. Acta* **1987**, *130*, 1; Norman, P. R.; Tate, A.; Rich, P. *Inorg. Chim. Acta* **1988**, *145*, 211.
(26) Marcel, L. M. P.; David, N. R. *J. Am. Chem. Soc.* **1980**, *102*, 7571.
(27) Brown, R. S.; Curtis, N. J.; Huguet, J. *J. Am. Chem. Soc.* **1981**, *103*, 6953.
(28) Brown, R. S.; Salmon, D.; Curtis, N. J.; Kusuma, S. *J. Am. Chem. Soc.* **1982**, *104*, 3188.
(29) Slebocka-Tilk, H.; Cocho, J. L.; Frakman, Z.; Brown, R. S. *J. Am. Chem. Soc.* **1984**, *106*, 2421.
(30) Palmer, D. A.; van Eldik, R. *Chem. Rev.* **1983**, *83*, 694, and references cited therein.
(31) Mahal, G.; van Eldik, R. *Inorg. Chem.* **1985**, *24*, 4165.
(32) Khalifah, R. G. *J. Biol. Chem.* **1971**, *246*, 2561.
(33) Gibbons, B. H.; Edsall, J. T. *J. Biol. Chem.* **1963**, *238*, 3504.
(34) Lindskog, S.; Thorshund, A. *Eur. J. Biochem.* **1968**, *3*, 456.
(35) Kernohan, J. C. *Biochim. Biophys. Acta* **1964**, *81*, 346.
(36) During the overall reaction for the hydration of CO_2, H^+ is released, whereas OH^- is produced during the dehydration of HCO_3^-.

Scheme II

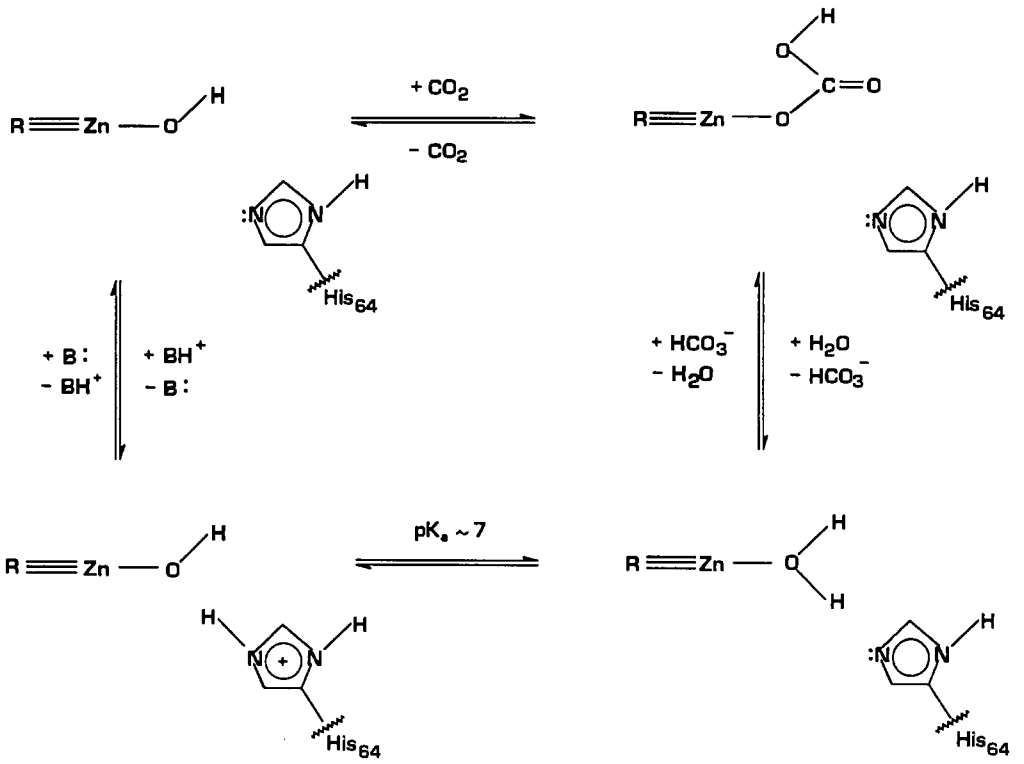

Scheme III

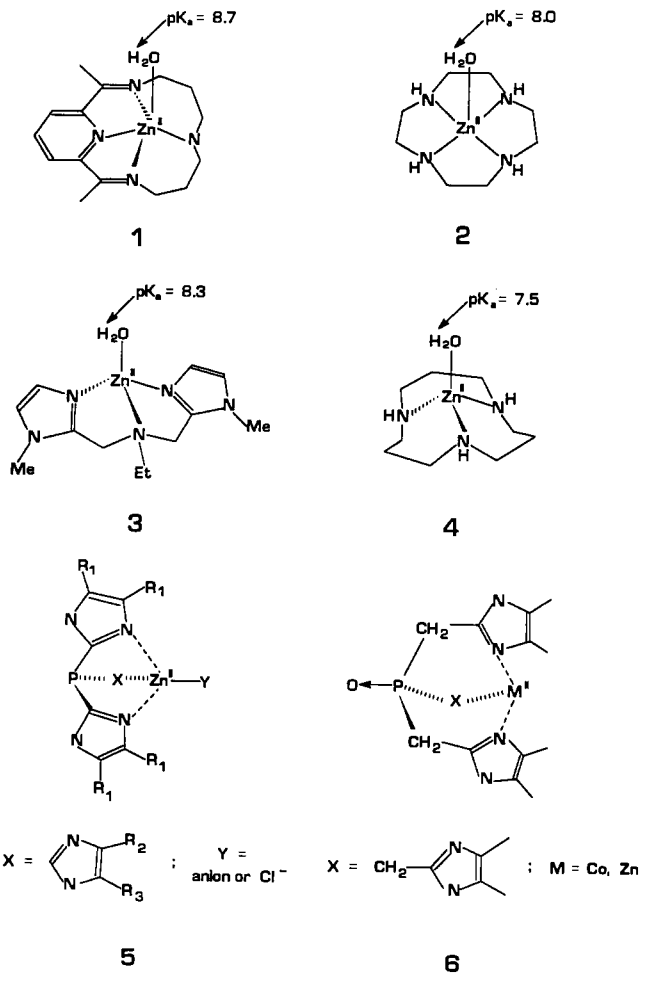

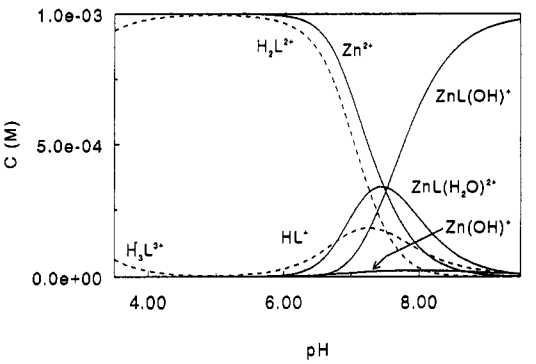

Figure 1. Distribution curves for various species in the pH range 3.5–9.0. Experimental conditions: temp = 25.0 °C, ionic strength = 0.1 M, and L = [12]aneN$_3$.

0.1 M $NaClO_4$) solution, and the absorbance time trace was recorded as described above. Plots of $V_{initial}$ versus $[Zn(II)]_T$ at a given pH gave good straight lines, from which the slope was used to calculate the second-order rate constant $(k^h_{cat})_{obs}$ or $(k^d_{cat})_{obs}$ for the catalyzed hydration of CO_2 or dehydration of HCO_3^-, respectively, and the intercept was used to calculate the first-order rate constant k^h_{obs} or k^d_{obs}, for the spontaneous hydration of CO_2 or dehydration of HCO_3^-, respectively.

pH Titration Procedure. An automatic titrator (Metrohm 702SM Titrino) coupled to a Metrohm electrode was used and calibrated according to the Gran method.[37] All titrations were carried out under Ar atmosphere, at 25.0 ± 0.2 °C, and at an ionic strength of 0.1 M ($NaClO_4$). For the determination of the ligand protonation constant two 50-mL stock solutions were prepared in which the total ligand and total acid concentrations were 1.00 and 3.50 mM and 2.00 and 7.13 mM, respectively. For the determination of the complex formation constant of Zn^{II}–L and the deprotonation constant of the bound water molecule in this complex, three 50-mL stock solutions containing the following total metal ion, ligand, and acid concentrations: 1.00, 1.00, 3.56 mM; 1.00, 2.00, 6.11 mM; and 1.00, 3.00, 9.16 mM, respectively. Duplicate titrations were performed with standardized 43.65 mM NaOH using 20 mL of each stock solution, for which the experimental error was below 1%. The titration data was fitted with the PSEQUAD program,[38] from which the distribution curve for the various species could be obtained (Figure 1).

(37) Gran, G. *Acta Chem. Scand.* **1950**, *4*, 559.
(38) David, J. L. *Computational Methods for the Determination of Formation Constants*; Plenum Press: New York, 1985, Chapter 8.

Results and Discussion

Distribution Curves for Species in Solution. The complex $[Zn^{II}L(OH)]_3(ClO_4)_3 \cdot HClO_4$ was characterized by a single-crystal X-ray analysis.[20] There are three $Zn^{II}([12]aneN_3)OH^+$ ions around a crystallographic 3-fold axis with the one $HClO_4$ molecule on this axis. pH titrations established that this trimeric complex in aqueous solution forms two $ZnL(OH)^+$ and one $ZnL(H_2O)^{2+}$ species as shown in (4). This assignment is also in

$$[Zn^{II}L(OH)]_3(ClO_4)_3 \cdot HClO_4 \xrightarrow{H_2O} 2ZnL(OH)^+ + ZnL(H_2O)^{2+} + 4ClO_4^- \quad (4)$$

agreement with the observed ^{1}H-NMR spectrum and the single pK_a value for **4**.[20] The complex is stable in a certain pH range and decomposes in others as shown in Figure 1. At pH < 6, only Zn(II) ions and free ligand are present in solution. Complex formation starts at pH > 6 and the following equilibrium constants were determined. These values are in close agreement with those

$$L + H^+ \rightleftharpoons HL^+ \quad K_1 = 10^{12.36} \quad (5)$$

$$HL^+ + H^+ \rightleftharpoons H_2L^{2+} \quad K_2 = 10^{7.52} \quad (6)$$

$$H_2L^{2+} + H^+ \rightleftharpoons H_3L^{3+} \quad K_3 = 10^{2.34} \quad (7)$$

$$Zn(II) + L \rightleftharpoons ZnL(H_2O)^{2+} \quad K_{ZnL} = 10^{8.65} \quad (8)$$

$$ZnL(H_2O)^{2+} \rightleftharpoons ZnL(OH)^+ + H^+ \quad K_a = 10^{-7.51} \quad (9)$$

cited elsewhere.[20] It follows from the distribution curves that under certain experimental conditions, free Zn(II) ions will be present in solution and may affect the kinetic measurements, an aspect that was studied in this investigation. The influence of $Zn(OH)^+$ at high pH can be neglected.

Hydration of CO_2. The kinetics of the uncatalyzed and catalyzed hydration of CO_2 were studied under the same experimental conditions in the pH range 6.0–9.0. The results for the uncatalyzed reaction, measured either directly in the absence of the catalyst or estimated from the data for the catalyzed reaction by extrapolation to zero catalyst concentration, are summarized along with literature data[32,33] in Figure 2. The reaction exhibits no significant pH dependence in the range 6.0–7.8 (see Figure 2a) and our mean values for k^h of 0.0301 ± 0.009 (●), 0.0281 ± 0.008 (○), and 0.0289 ± 0.008 (□) s^{-1}, obtained in three different ways, are in good agreement with each other and with the literature data.[32,33] According to the overall reaction scheme given in (10),[32,33] the observed hydration rate constant in neutral solutions

$$\begin{array}{ccc} H^+ + HCO_3^- & \underset{k_{21}}{\overset{k_{12}}{\rightleftharpoons}} & H_2CO_3 \\ k_{13}\downarrow\uparrow k_{31} & & k_{23}\downarrow\uparrow k_{32} \\ & CO_2 + H_2O & \end{array} \quad (10)$$

is given by $k^h = k_{31} + k_{32}$. When the pH is increased to 9.0, the OH^--catalyzed reaction (11) contributes significantly toward the

$$CO_2 + OH^- \xrightarrow{k_{OH}} HCO_3^- \quad (11)$$

$$k^h_{obs} = k^h + k_{OH}[OH^-] \quad (12)$$

observed hydration rate constant given in (12). The plot of k^h_{obs} versus $[OH^-]$[39] given in Figure 2b exhibits a good linear dependence from which it follows that $k_{OH} = (7.9 \pm 0.6) \times 10^3$ M^{-1} s^{-1} and $k^h = 0.047 \pm 0.007$ s^{-1}. The results in Figure 2 indicate a good agreement between the different ways in which k^h_{obs} was determined and also with the cited literature data.[32,33] Our k_{OH} value is close to that obtained from conductivity measurements,[40] viz. 8.5×10^3 M^{-1} s^{-1}.

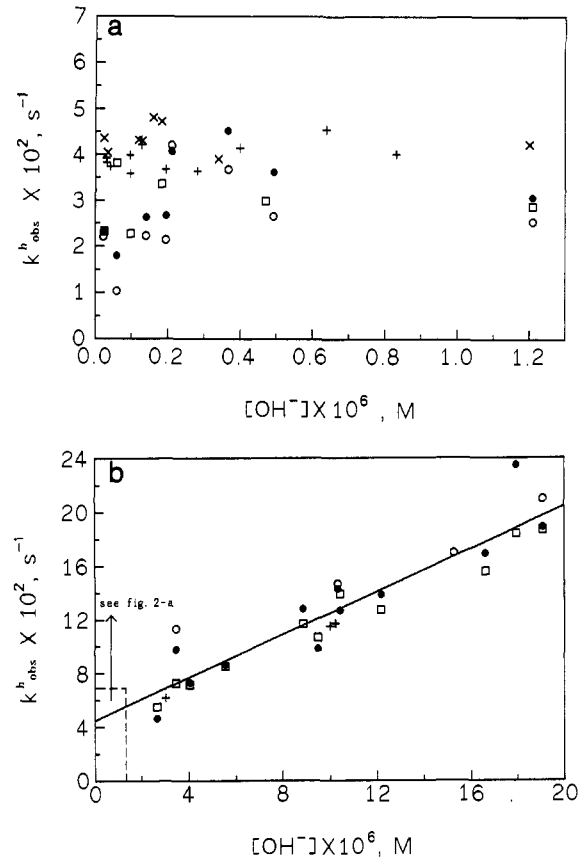

Figure 2. Summary of rate constants for the hydration of CO_2 as a function of $[OH^-]$ in the pH range 6.0–9.0 at 25 °C. (Data for the lower concentration range are reported in part a.) Experimental conditions: For data from this study (●, ○, □), temperature = 25.0 °C, ionic strength = 0.11 M, [indicator] = (2–5) × 10^{-5} M, and [buffer] = 50 mM. For literature data (×, +) see refs 32 and 33. Key: (●) data obtained directly from uncatalyzed hydration rates; (○) data extrapolated from Figure 4; (×) data reported in ref. 33; (+) data reported in ref. 32; (□) data obtained from initial slopes of kinetic traces.

Typical kinetic traces observed for the uncatalyzed and Zn(II) catalyzed hydration of CO_2 using different buffer-indicator pairs over the pH range 6.1–9.0, are reported in Figure 3 (supplementary material). The kinetic traces in Figure 3a,b clearly demonstrate the catalytic effect of Zn^{II}–[12]aneN$_3$, and indicate that the overall absorbance change ($A_0 - A_e$) is very similar for both reactions, i.e. the same concentration of H^+ is released during the reactions within the experimental error limits. On increasing pH, the kinetic traces exhibited more of a two exponential behavior, but 10% of the overall reaction fitted to a single exponential decay was used to obtain $V_{initial}$. Some typical plots of $V_{initial}$ versus $[Zn(II)]_T$ are shown in Figure 4, from which it follows that the initial hydration rate varies linearly with the total Zn(II) concentration and increases significantly on increasing pH. The corresponding values of $(k^h_{cat})_{obs}$ are summarized in Table I, and the data are plotted as a function of pH in Figure 5. The pH range was

(39) For the estimation of the OH^- concentration, the ion product of water was measured as 1.97×10^{-14} using a literature procedure[37] for our experimental conditions, and was taken as 1.66×10^{-14} (Busey, R. H.; Mesmer, R. E. *J. Chem. Eng. Data* **1978**, *23*, 175) for the literature data.

(40) Sirs, J. A. *Trans. Faraday Soc.* **1958**, *54*, 201.

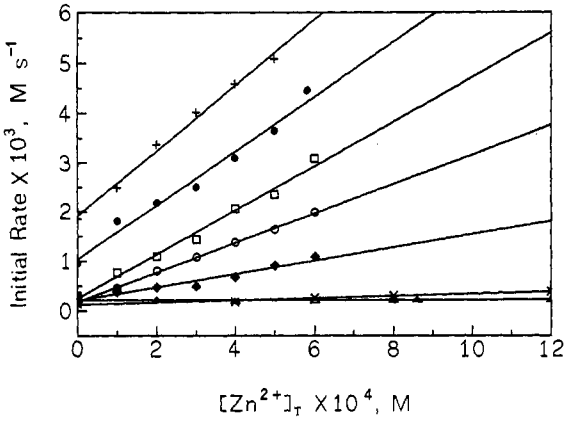

Figure 4. Typical plots of initial rate versus $[Zn(II)]_T$ for the hydration of CO_2 as a function of pH at 25 °C. For experimental conditions see Table I. Key: (△) pH = 6.05; (×) pH = 6.47; (○) pH = 7.40; (□) pH = 7.79; (♦) pH = 7.00; (●) pH = 8.24; (+) pH = 8.89.

Table I. Summary of the Second-Order Rate Constants, $(k^h_{cat})_{obs}$, for the Zn(II)-Catalyzed Hydration of CO_2 as a Function of pH[a]

buffer	10^5[indicator], M	pH[b]	$(k^h_{cat})_{obs}$, M^{-1} s^{-1}
Mes	2.21	6.05	0.14 ± 0.92[c]
Bis-tris	3.02	6.47	3.3 ± 0.7[c]
Mops	4.31	6.85	128 ± 16
	4.31	7.00	136 ± 15
	4.31	7.03	146 ± 11
Hepes	2.20	7.27	224 ± 17
	2.20	7.40	284 ± 12
Hepps	4.18	7.79	453 ● 24
Taps	4.18	8.24	511 ± 34
Ampso	2.42	8.89	556 ± 69
	2.42	8.99	578 ● 56
Ches	2.42	9.12	562 ● 41

[a] Experimental conditions: [buffer] = 50 mM; temperature = 25.0 °C; ionic strength = 0.135 M; $[CO_2]$ = 12.3 mM or 9.85 mM. [b] Mean pH calculated from pH measurements before and after the reaction. The pH difference was never more than 0.2 units. [c] According to the distribution curves in Figure 1, there is nearly no complex formed at pH 6.05 and very little (<5 %) at pH 6.47. Both of these data points were not included in the calculation of k^h_{cat}.

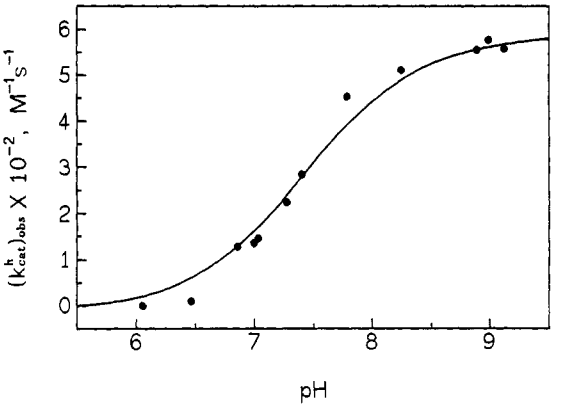

Figure 5. Plot of $(k^h_{cat})_{obs}$ versus pH. For experimental conditions see Table I. The solid line was calculated on the basis of the mechanism outlined in eq 14—see Discussion.

restricted by the decomposition of the complex at lower pH, and the interference of the spontaneous base-catalyzed hydration reaction at pH > 9.0, where the initial rate method could not be employed since the buffer factor could not be kept constant under such conditions due to the complication of carbonate formation. The effect of free Zn(II) ions on the reaction was checked at pH = 6.85, but no catalysis was observed.

The sigmoid shaped curve is characteristic for a kinetic process controlled by an acid–base equilibrium and exhibits an inflection around a pH of 7.4, i.e. the pK_a value of 4. Thus the Zn^{II}–

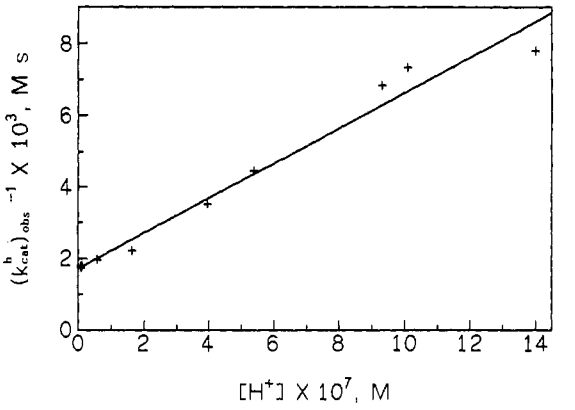

Figure 6. Plot of $(k^h_{cat})_{obs}^{-1}$ versus $[H^+]$ for the data in Table I.

[12]aneN$_3$ complex must play a crucial role in the catalyzed hydration of CO_2, similar to that found for related reactions.[20,21] The pH dependence of $(k^h_{cat})_{obs}$ can be accounted for in terms of the mechanism outlined in (13), which is based on the principle

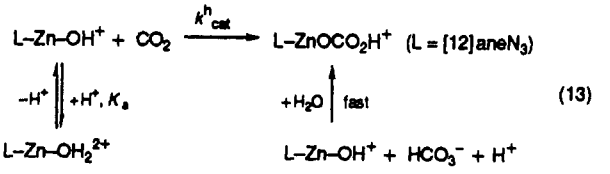

(13)

that only the hydroxo complex can react with CO_2 in order to catalyze the hydration reaction.[30,41] In this scheme it is assumed that the produced bicarbonate complex is unstable and rapidly aquates to bicarbonate and the aqua complex, which deprotonates under these conditions to the hydroxo species. It is reasonable to assume that no stable bicarbonate complex is formed since the release of protons was observed during the reaction. In addition, no evidence whatsoever could be found for the presence of such a complex.

The rate law for the suggested CO_2 hydration mechanism is given in (14), from which it follows that a plot of $(k^h_{cat})_{obs}^{-1}$

$$(k^h_{cat})_{obs} = k^h_{cat} K_a/([H^+] + K_a) \quad (14)$$

versus $[H^+]$ should be linear. The data in Table I are plotted accordingly in Figure 6, from which it follows that K_a = (3.5 ± 0.4) × 10^{-8} M and k^h_{cat} = 581 ± 64 M^{-1} s^{-1} at 25.0 °C. Indeed this K_a value, viz. pK_a = 7.45 ± 0.10, is very close to that determined for the aqua complex above and underlines the validity of the suggested mechanism. The values of K_a and k^h_{cat} were used to calculate the sigmoid curve in Figure 5, which fits the experimental data rather well.

Dehydration of HCO_3^-. A few typical kinetic traces for the catalyzed dehydration of HCO_3^- are reported as a function of pH in Figure 7 (supplementary material). The traces clearly show that the dehydration of HCO_3^- can only be studied over a limited pH range due to the interference of the reverse hydration reaction especially at higher pH (see initial absorbance decrease associated with the hydration reaction in Figure 7d). The kinetics of the uncatalyzed and catalyzed reactions were studied under similar experimental conditions. Kinetic data obtained directly for the uncatalyzed reaction are in close agreement with those extrapolated from the catalyzed reaction at zero Zn(II) concentration, as indicated by the plot of $V_{initial}$ versus $[H^+]$ in Figure 8. The rate law for the uncatalyzed dehydration reaction according to the overall scheme in (10) is given by eq 15, where $k^d = k_{13} + k_{23}k_{12}/k_{21}$. The $[HCO_3^-]$ was calculated from the known acid

(41) (a) Chaffee, E.; Dasgupta, T. P.; Harris, G. M. *J. Am. Chem. Soc.* **1973**, *95*, 4147. (b) Schwarzenbach, G. *Helv. Chim. Acta* **1957**, *40*, 907.

$$V_{initial} = k^d[HCO_3^-][H^+] \quad (15)$$

dissociation constants,[42] and the resulting value for k^d from Figure 8, viz. $(5.9 \pm 0.5) \times 10^4$ M^{-1} s^{-1}, is in good agreement with a value of $(5.85 \pm 0.06) \times 10^4$ M^{-1} s^{-1} reported in the literature.[33]

The dehydration reaction is only slightly catalyzed by the model Zn(II) complex (Figure 9), and the effect decreases with increasing pH. The latter trend suggests that the aqua complex must be the reactive catalytic species. The pH range was once again restricted by the decomposition of the Zn(II) complex at lower pH and the interference of the hydration reaction of CO_2 at higher pH. The kinetic data were fitted to the suggested mechanism in (16), for which the corresponding rate law is given

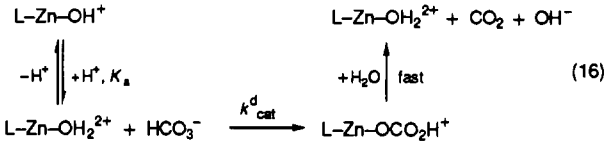

(16)

in (17). Accordingly, a plot of $(k^d_{cat})_{obs}^{-1}$ versus $[H^+]^{-1}$ should

$$(k^d_{cat})_{obs} = k^d_{cat}[H^+]/([H^+] + K_a) \quad (17)$$

be linear, which is the case for the experimental data (see Figure 10). The error in the measurements increases with decreasing $[H^+]$ due to the restrictions mentioned above. From this data fit it followed that $k^d_{cat} = 4.8 \pm 0.7$ M^{-1} s^{-1} and $K_a = (5.3 \pm 0.8) \times 10^{-8}$ M; i.e. $pK_a = 7.29 \pm 0.13$. The latter value is rather close to that found from the pH dependence of the catalyzed hydration reaction of CO_2 when the limited pH range is taken into account, and underlines the validity of the suggested mechanism. Again it was checked that free Zn(II) ions had no effect on the reaction, such that the observed catalytic effect must be due to the complex **4**.

Overall Catalytic Mechanism. It follows from the above reported data that the model Zn^{II}–[12]$aneN_3$ complex exhibits a catalytic activity for both the hydration of CO_2 and dehydration of HCO_3^-, which is controlled by the pH of the solution. In acidic pH, the aqua complex exhibits a slight catalytic activity on the dehydration of HCO_3^- in which the rate-determining step is substitution of the labile water molecule by HCO_3^-, followed by the rapid decarboxylation of the coordinated bicarbonate molecule as found for many model bicarbonate complexes.[30] In basic solution, the less labile hydroxo complex is able to catalyze the hydration of CO_2, for which the CO_2 uptake reaction (see (13)) is the rate-determining step and is followed by the rapid aquation reaction of the bicarbonate complex. Thus the model complex is the first example to mimic the catalytic activity of CA in that there is a competition between uptake/decarboxylation reactions on the one hand, in which no Zn–O bond cleavage occurs, and substitution reactions on the other hand, where Zn–O bond cleavage does occur. In all the model complexes studied before[30,31] either only uptake/decarboxylation reactions or only substitution reactions were observed, depending on the lability of the metal center. For nonlabile octahedral complexes of Co(III), Rh(III), Ir(III), and Cr(III),[30] only CO_2 uptake and decarboxylation of coordinated HCO_3^- were observed, whereas for labile square planar complexes of Pd(II)[31] only substitution of coordinated water by HCO_3^- and the reverse were observed. Thus the model Zn(II) complex exhibits the unique property of a labile water molecule that can undergo a substitution reaction with HCO_3^- and a nonlabile hydroxy ligand that can undergo a CO_2 uptake reaction. Consequently, coordinated bicarbonate has the choice to either be substituted during the reverse aquation reaction, or to loose CO_2 during the reverse decarboxylation reaction. The overall catalytic mechanism is summarized in Scheme IV. The deprotonation of L–Zn–OCO_2H^+ is not included since this could lead to a stable L–Zn–OCO_2 species, as found for the other model systems,[30,31] but no evidence for the formation of such a product was found in this study. It is likely that such a complex could also be fairly labile and undergo a rapid substitution reaction.

(42) The dissociation constants for carbonic acid are well-known at zero ionic strength,[41] but data in the range 0.01–0.5 M ionic strength are scarce. We estimated $pK_1 = 6.14$ at 0.1 M ionic strength from the literature (Nasanen, R.; Merilanen, P.; Leppanen, K. *Helv. Chim. Acta* **1961**, *15*, 915) and took $pK_2 = 9.8$ from ref 41.

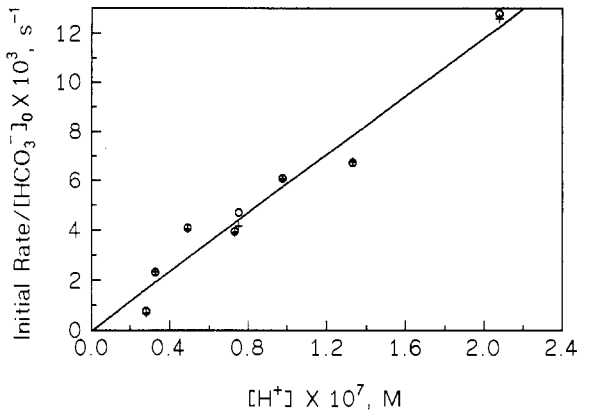

Figure 8. Effect of $[H^+]$ on the initial rate of the spontaneous dehydration of HCO_3^-. Experimental conditions: [buffer] = 50 mM; ionic strength = 0.1 M; $[NaHCO_3] = 6 \times 10^{-3}$ M; [indicator] = $(2–5) \times 10^{-5}$ M; temperature = 25.0 °C. Key: (+) data measured directly from uncatalyzed hydration rates; (O) data extrapolated from Figure 9.

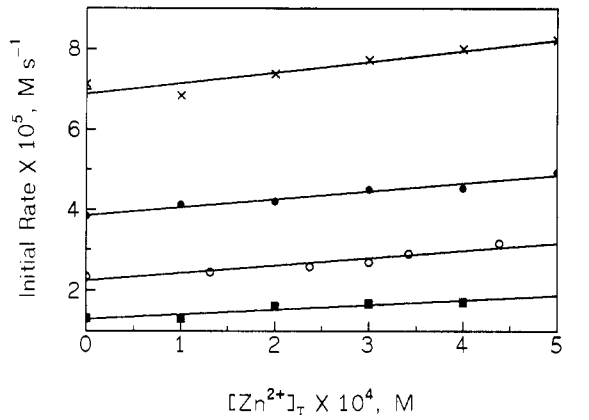

Figure 9. Plots of initial rate versus $[Zn(II)]_T$ for the dehydration of HCO_3^- as a function of pH at 25 °C. For experimental conditions see Figure 7. Key: (■) pH = 7.56; (O) pH = 7.13; (●) pH = 6.88; (×) pH = 6.68.

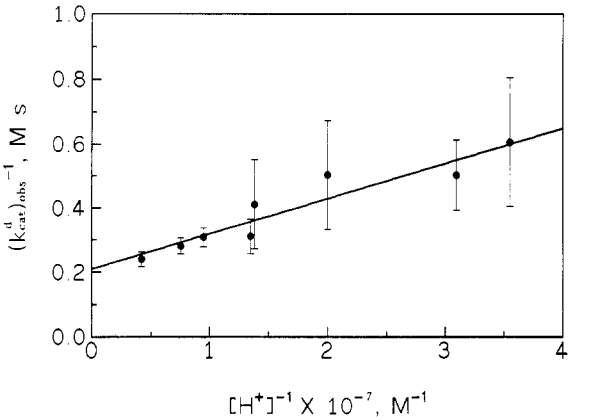

Figure 10. Plot of $(k^d_{cat})_{obs}^{-1}$ versus $[H^+]^{-1}$ for the catalyzed dehydration of HCO_3^-. For experimental conditions see Figure 7. Experimental data are for the pH range 6.68–7.56. $[H^+]$ concentrations were calculated from the mean pH value measured before and after the reaction, which never differed more than 0.14 pH units.

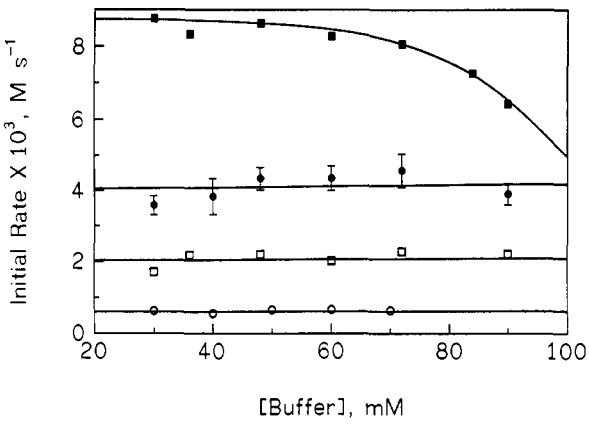

Figure 11. Effect of buffer concentration on the spontaneous and catalyzed hydration of CO_2. Experimental conditions: $[CO_2]$ = 9.8 mM; ionic strength = 0.11 M; [buffer]/[*m*-cresol purple] = 1438; λ = 578 nm; temperature = 25 °C. Key: (○) Hepps in the absence of Zn(II), pH = 7.84; (□) Tricine in the absence of Zn(II), pH = 7.96; (●) Hepps in the presence of 5×10^{-5} M Zn(II), pH = 7.84; (■) Tricine in the presence of 5×10^{-5} M Zn(II), pH = 7.96.

Scheme IV[a]

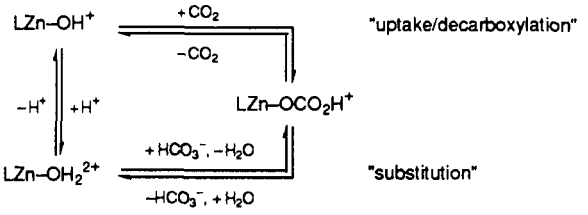

[a] L = [12]ane N_3.

In Scheme IV the protonation/deprotonation of the Zn(II) complex (reaction 9) involves proton transfer. Furthermore, proton transfer (Lipscomb mechanism) or oxygen transfer (Lindskog mechanism)[43] must be involved during CO_2 uptake by $LZn–OH^+$ to produce $LZn–OCO_2H^+$ and during the reverse decarboxylation reaction. The location of the proton on the bicarbonate complex, viz. $LZn–O(H)CO_2^+$ or $LZn–OCO_2H^+$, is crucial in determining the stability of the Zn–O and O–C bonds, which in turn controls the "uptake/decarboxylation" and "substitution" steps in Scheme IV. Such proton-transfer processes could be affected by the buffer employed, and for this reason the effect of the buffer concentration on the uncatalyzed and catalyzed hydration of CO_2 was investigated. For this purpose different types of buffers with different functional residues, viz. $>^+NH–CH_2–CH_2–SO_3^-$ and $>^+NH–CH_2–COO^-$, were selected and the results are summarized in Figure 11. It follows that in most cases the buffer concentration had no significant influence on the initial rate of the reaction for both the spontaneous and catalyzed processes at buffer concentrations higher than 30 mM. This clearly shows that proton transfer between the zinc-bound water molecule and the medium is too fast to be the rate-determining step under our experimental conditions. In the case of Tricine at concentrations higher than 70 mM, a significant decrease in the catalytic reactivity of the model complex could be detected. It is obvious that Tricine reacts with the Zn(II) complex under such conditions and suppresses its reactivity. The buffer concentration of 50 mM selected in the present study is such that no limiting effect due to proton-transfer reactions can be expected.

The investigated model complex exhibits a moderate catalytic effect on the hydration of CO_2. Our value for k^h_{cat} of 581 ± 64 M^{-1} s^{-1} at 25 °C is on the higher limit of the values reported for CO_2 uptake by one kind of model complexes studied before.[30,45] These complexes all involve a single coordinated OH^- ligand, similar to that of complexes **1**–**4**. A value of 590 ± 30 M^{-1} s^{-1} was reported for CO_2 uptake by $Cu(gly)_2OH$, but this complex is characterized by a pK_a value of 9.4.[44] Furthermore, the present model complex **4** is significantly more reactive than the $Zn(CR)OH^+$ complex (CR = Me_2pyo[14]trieneN_4), for which a CO_2 uptake rate constant of 225 ± 23 M^{-1} s^{-1} was reported.[45] If we exclude the native role of the hydrophobic pocket, the proton relay and other structural factors in CA, our results favor the $Zn^{II}–OH^+$ mechanism.[1] Both the low pK_a value around 7 and the tetrahedral ligand arrangement are essential for this mechanism. This ligand arrangement provides more space for the entering nucleophile than in the case of five or six coordinated ligands. For another series of tris(imidazole) complexes (**5** and **6**), maximum rate constants of 900 (**5**, $R_1 = R_2 = R_3 = CH(CH_3)_2$), 1500 ($R_1 = CH(CH_3)_2$, $R_2 = R_3 = H$), and 2700 M^{-1} s^{-1} ($R_1 = R_2 = R_3 = CHCH_2CH_3$) were reported.[29] Although these complexes exhibit a higher catalytic reactivity than **4**, they failed to mimic the characteristic pH profile for both the hydration and dehydration reactions as suggested for CA by many groups.[1-13] Instead, these complexes showed some acid catalysis for the hydration reaction. The high catalytic effect observed for these complexes[29] may be due to the hydrophobic environment of the metal center. It remains, however, important to note that the model complex **4** investigated in this study catalyzes both the hydration and dehydration reactions, and exhibits the characteristic pH dependence reported for the catalytic activity of CA.

We conclude that although the model complex **4** can mimic the catalytic activity of CA for both the hydration of CO_2 and dehydration of HCO_3^- very nicely, its catalytic activity is very moderate. The unique combination of the distorted tetrahedral geometry and the low pK_a value of 7.5 certainly play an important role in the catalytic paths for reaction 1. However, the importance of the hydrophobic pocket, proton relay, and other structural features of CA cannot be accounted for by this work. The large difference in reactivity between CA and the model complex **4** may be related to an effective preassociation of CO_2 within the hydrophobic pocket in CA,[9,11,13,47] i.e. close to the reactive site, something that is not possible in our model complex. If this preassociation is characterized by a large binding constant of 10^4 M^{-1}, it can account for the 4 orders of magnitude difference observed in the catalytic activity during the hydration of CO_2. Such a large preassociation constant will require a very specific interaction of CO_2 with a functional group within the hydrophobic pocket. Formation of HCO_3^- at the active site will then lead to a rapid release of HCO_3^- due to the significantly weaker interaction with the hydrophobic pocket. In the case of the dehydration of HCO_3^-, an effective preassociation with the hydrophilic pocket could account for the high catalytic reactivity. It is therefore essential that further work on model systems will have to include ligands that create a hydrophobic environment for the preassociation of HCO_3^-, in order to be able to mimic the overall process and to resolve the structural details of the important intermediate species.

Acknowledgment. R.v.E. gratefully acknowledges financial support from the Deutsche Forschungsgemeinschaft, Fonds der Chemischen Industrie, and the Volkswagen-Stiftung.

Supplementary Material Available: Typical kinetic traces for the spontaneous and catalyzed hydration of CO_2 (Figure 3a–f) and for the dehydration of HCO_3^- (Figure 7a–d) (4 pages). Ordering information is given on any current masthead page.

(43) Miguel, S.; Agusti, L.; Miguel, D.; Juan, B. *J. Am. Chem. Soc.* **1992**, *114*, 869.
(44) Dasgupta, T. P.; Harris, G. M. *J. Am. Chem. Soc.* **1977**, *99*, 2490.
(45) Woolley, P. *Nature* **1975**, *258*, 677.
(46) Kogut, K. A.; Rowlett, R. S. *J. Biol. Chem.* **1987**, *262*, 16417.
(47) Aqvist, J.; Fothergill, M.; Warshel, A. *J. Am. Chem. Soc.* **1993**, *115*, 631.